

## Echo-Planar Imaging of Diffusion and Perfusion\*

ROBERT TURNER,† DENIS LE BIHAN,‡ AND A. SCOTT CHESNICK§

†Biomedical Engineering and Instrumentation Program, National Center for Research Resources;  
‡Department of Diagnostic Radiology, Warren G. Magnuson Clinical Center; and §National Heart,  
Lung and Blood Institute, National Institutes of Health, Bethesda, Maryland 20892

Received February 1, 1991; revised February 26, 1991

Use of the Stejskal-Tanner sequence for performing diffusion images in the human brain tends to be complicated by the presence of artifacts caused by voluntary or involuntary, sometimes pulsatile, motion. We describe the implementation of the technique of echo-planar diffusion imaging, which avoids these artifacts and allows reproducible quantitative values of the diffusion coefficient to be measured *in vivo*. The effects of perfusion are easily visible in a phantom containing a gel. The results for human brain show a significant "perfusion fraction" in grey matter, consistent with an extracellular, possibly microvascular, volume of about 10%. © 1991 Academic Press, Inc.

### INTRODUCTION

The usual Stejskal-Tanner technique for sensitizing a multipulse MR imaging sequence to microscopic flows also makes it very sensitive to bulk motions, such as pulsations related to the cardiac cycle, involuntary twitches, and CSF flow. Imaging hardware must be very stable, and eddy currents in surrounding conducting structures caused by the unusually large magnetic field gradients ( $I$ ) can seriously impair image interpretability. Large eddy currents with short time-constants rule out any kind of rapid imaging technique.

With the aid of special-purpose gradient coils, either self-shielded or built on a small diameter, and the use of echo-planar imaging (2-5) in which the entire image data set is captured in less than 0.1 s, these problems are completely avoided. No trace of motion artifact is observable in heavily diffusion-weighted images of the human or cat brain.

### PULSE SEQUENCES AND HARDWARE

Echo planar imaging may be sensitized to flow and diffusion in precisely the same way as conventional spin-echo or gradient-echo imaging sequences. For a spin-echo sequence, a pair of diffusion gradient pulses of the same polarity may be placed on either side of the refocussing  $180^\circ$  pulse (6), or if a gradient-echo sequence (7) is desired, a bipolar pair of gradients may be placed before signal acquisition (Fig. 1).

\* Presented at SMRM Workshop on Future Directions in MRI of Diffusion and Microcirculation, Bethesda, MD, June 7 and 8, 1990.

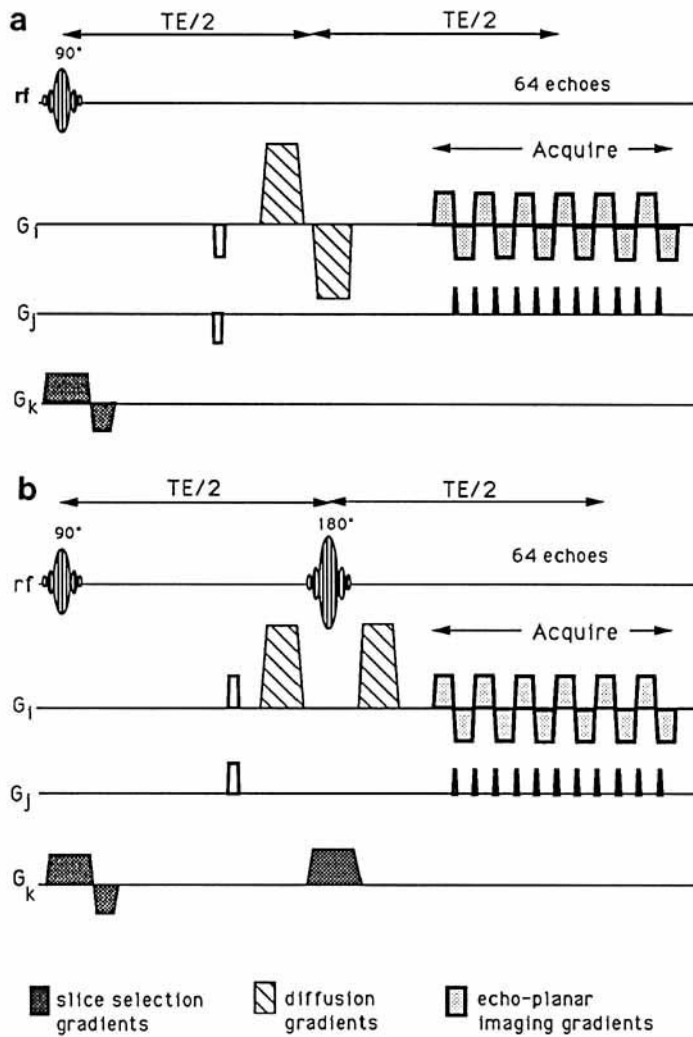


FIG. 1. Diffusion-weighted echo-planar imaging sequences: (a) Gradient-echo MBEST, (b) Spin-echo MBEST.

The major problems involved in implementing echo planar diffusion imaging stem from the same causes; the shortness in tissue of the transverse relaxation time  $T_2$  and the inhomogeneity-related dephasing time  $T_2^*$ . If too long a time elapses between the excitation of the spin system and the acquisition of the data, no signal remains to be observed. Thus the large excursions of the trajectory in  $k$ -space needed in order to provide reasonable resolution must be traversed very rapidly, typically in 50–100 ms; hence large, rapidly switched gradients must be provided. Furthermore, the diffusion gradients must be of short duration, less than 40 ms per lobe, say. Given typical tissue values for  $D$  of  $0.5\text{--}1.0 \times 10^{-3} \text{ mm}^2 \text{ s}^{-1}$ , this implies that gradient strengths of at least

10 mT m<sup>-1</sup> are desirable for this gradient too if a significant diffusion-related signal attenuation is to be obtained.

Both of the IVIM-EPI sequences described above have been successfully implemented on a 1.5-T whole-body GE Signa scanner (4), and on 2.0- and 4.7-T medium-bore GE CSI systems (8, 9). On all of these imaging machines 128 × 128 images of long T2 phantoms have been obtained, but the data acquisition rate available makes the acquisition time (i.e., the digitizing window duration) too long for *in vivo* work at this resolution. The studies reported here were performed at 64 × 64 resolution. Later work (5) has been performed using a GE Signa system retrofitted with fast imaging gradients and acquisition hardware (Advanced NMR Systems, Inc., Woburn, MA).

A further essential precaution, for the medium bore magnets, was to obtain the best shim possible with the magnet used. Fortunately, the standard shim on the Signa was entirely adequate for EPI with the acquisition time used, and no special shimming was needed.

#### WHOLE-BODY IMPLEMENTATION

Normal commercial whole-body gradient hardware gives gradients up to 10 mT m<sup>-1</sup>, but the switching time of 0.5–1.0 ms is far too slow to allow the 64 or more gradient switches to be made in the time available before the signal decays. A switching time of 400 μs or less is required for EPI to be feasible, and a maximum gradient strength of about 20 mT m<sup>-1</sup> is needed to achieve an in-plane resolution of 2.5 × 2.5 mm.

These stringent gradient requirements may be met by using the existing gradient coils while increasing the number or power of the gradient current amplifiers, so that a larger current is made available, along with a higher maximum voltage to raise the current faster to its desired value. This is the strategy currently employed by Mansfield and his team (10) for whole-body imaging. The alternative is to build a small special-purpose gradient coil that fits over the head and which can be designed to give much greater efficiency and smaller inductance than standard whole-body gradient coils. In this case no additional gradient power supplies are required.

Using the target field coil design method (11) a z-gradient coil with 20 cm diameter volume of linear gradient, with 100 μH inductance, and 40 mT m<sup>-1</sup> (100 A)<sup>-1</sup> efficiency was designed. This coil is compact enough to fit round the head in such a way that the shoulders are barely touching the end, yet the entire brain can be imaged without distortion. Transverse gradient coils which have such excellent specifications are not feasible (12), but reasonably compact designs of about half this efficiency for the same inductance have been built.

An rf coil was built inside the gradient coil former. To prevent undue loading by the gradient coil, and the production of secondary parasitic resonances, pieces of copper foil were judiciously placed in order to screen the gradient wires themselves from the rf fields. These were tuned to create an anti-resonance mode in the gradient coils, thus preventing inductive coupling to the rf coil. A simple four element rf saddle coil was used, with a balanced capacitive-match feed, which gave, after careful tuning, a volume of homogeneous field of about 15 cm diameter. The coil was also equipped with copper foil guard rings to avoid excessive rf electric fields within it, which in the

presence of a patient's head causes detuning, reduction in  $Q$ , and unacceptable power deposition.

#### MEDIUM BORE IMPLEMENTATION

Results from the 2-T GE CSI imaging system, of magnet clear bore 45 cm diameter, were obtained using a GE "Acustar 260" set of actively shielded gradients (1, 13, 14), which gave a maximum gradient of  $40 \text{ mT m}^{-1}$ , with a rise-time of  $170 \mu\text{s}$ . At  $64 \times 64$  resolution, this enabled a minimum field of view of 40 mm to be achieved, giving a pixel size of  $0.625 \times 0.625 \times 2.0 \text{ mm}$ . A small birdcage rf coil, of 12 cm i.d., was used for work with phantoms and cats, and the EPI sequence was implemented in a way similar to that detailed in Refs. (8) and (15).

#### DIFFUSION AND PERFUSION EXPERIMENTS IN PHANTOMS

The reliability of the IVIM-EPI sequences was established, both on the 2-T CSI system and on the 1.5-T Signa, using experiments on water-containing phantoms. Most of this work was done on the 2-T CSI system. A bottle containing undoped water was imaged with varying diffusion gradients. The signal from a given region of interest was plotted against gradient  $b$ -factor (4) and found to agree with the theoretical predictions, with a value of the diffusion constant close to that found by the majority of workers (16, 17). Next a flow phantom was tested, containing a Sephadex 50–150 chromatography gel, through which a very slow current of water could be passed, simulating perfusion in a capillary bed. The results showed a dramatic effect on the signal, as predicted by IVIM theory (18) when the water flow was switched on. It should be noted in passing that a waiting period of at least 30 min after flow is started is needed in order to establish a steady state, before taking measurements. The attenuation dependence on  $b$ -factor changes from a single exponential with no flow to a curve which is fitted well by a biexponential, with the two exponents well separated in magnitude.

#### STUDIES IN HUMAN BRAIN

Echo planar diffusion imaging was successfully carried out, on volunteers and patients, using a GE Signa 1.5-T imaging system and the small head coil described above. The rate of switching of the current in this coil was restricted so that a maximum rate of magnetic field variation of  $16 \text{ T s}^{-1}$  was experienced by the subject, well below the maximum specified in FDA guidelines. No nonauditory sensory effects were reported by any subject. The acoustical noise generated during switching was sufficiently loud that all subjects wore earplugs for comfort.

Typically a series of 8 or 16 images of a single slice was collected, with different diffusion gradient strengths. A repetition time of 4 s was used. Each imaging shot was usually preceded by a phase reference shot with the phase-encode gradient switched off, which was used to correct the echo spacing and hence to avoid the "Nyquist ghost" artifact which otherwise appears halfway across the field of view from the image (4). Even with the highest diffusion gradient used,  $38 \text{ mT m}^{-1}$  for a duration of 20 ms per lobe, no motion artifact could be seen on the image. Images were normally obtained using the spin-echo MBEST (8, 9) sequence, echo time TE 100 ms, 16 cm FOV, 10

mm slice thickness,  $64 \times 64$  pixel matrix. With no diffusion weighting, the single-shot signal:noise ratio in grey matter was about 50. The image contrast was dominated by tissue T2 variations, as shown in Fig. 2.

Grey and white matter could be clearly distinguished, and the anisotropy of the diffusion coefficient in white matter (4, 19, 20) was easily observable, the intensity from fibers running perpendicular to the diffusion gradient decreasing more slowly than that of fibers parallel to the gradient.

To give an idea of the reproducibility of these results, Fig. 3 shows a comparison of data from regions of interest in two volunteers, each selected to lie in the amygdala. The data were scaled so that the intercepts of the log-linear fits to each set were zero. It is clear that there is excellent agreement. Figure 4 shows averaged data from three sets of images acquired in the same session from Volunteer 1. The scatter is evidently reduced; the SNR for the first point is about 170. The Levenberg-Marquardt nonlinear least-squares fit algorithm gives a good fit to a biexponential. Values of the perfusion

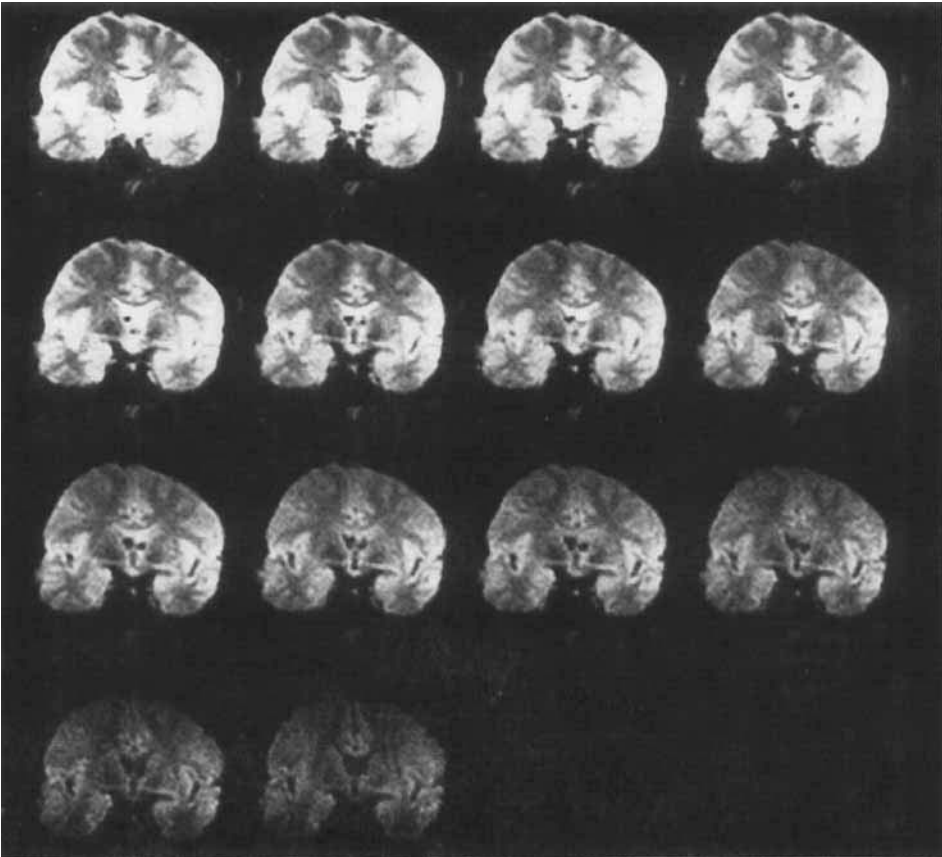


FIG. 2. Set of 14 diffusion-weighted  $64 \times 64$  coronal EPI images of volunteer head. FOV = 16 cm, slice thickness = 10 mm, TE = 100 ms, TR = 4 s, total acquisition time per image = 50 ms. The diffusion gradient duration was 20 ms/lobe, and the maximum gradient used was  $38 \text{ mT m}^{-1}$ .

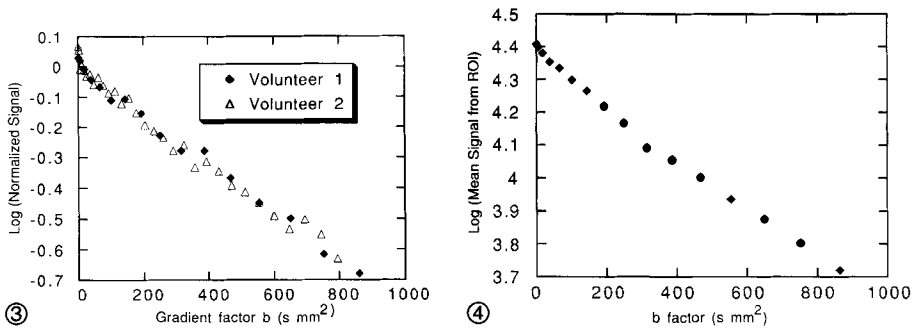


FIG. 3. Comparison of attenuation curves for two subjects, Volunteers 1 and 2, for ROIs selected in the amygdala, each about 4 pixels in size. The data are normalized by dividing by the intercept of a straight line fitted to the log of the data points versus the  $b$  factor. The scatter reflects the signal:noise ratio in single-shot images.

FIG. 4. Plot of mean signal attenuation, using three sets of images from Volunteer 1. Each group of three for a given value of  $b$  was acquired within 12 s. The image data were averaged after the modulus images had been reconstructed separately, so that no phase cancellation could occur. Cardiac gating was not used. The curvature in this plot indicates that a single exponential fit is inappropriate.

fraction  $f = 11 \pm 4\%$ , the diffusion coefficient of  $0.66 \pm 0.5 \times 10^{-3} \text{ mm}^2 \text{ s}^{-1}$ , and the pseudo-diffusion coefficient of  $5 \pm 2 \times 10^{-3} \text{ mm}^2 \text{ s}^{-1}$  were deduced. These are consistent with the IVIM theory and suggest a two-compartment model with 10% of the signal coming from the compartment with the larger diffusion coefficient.  $D^*$  is somewhat too large to be easily identified with CSF or extracellular fluid, though this interpretation cannot be excluded.

The work reported in (5) used a maximum value of  $b$  of about 300, considerably lower than the value of 800 used in the present work. At  $b = 300$ , the asymptotic slope has not yet been reached, which may explain the rather larger estimates of  $D$  given in Ref. (5). Subsequent work by this group (21), extending to larger  $b$  values has given results in good agreement with those presented here.

#### CONCLUSIONS

Single-shot echo planar imaging enables precise, reproducible measurements of diffusion coefficients of human brain tissue *in vivo*, without confusing motion artifacts. The implications for effective and timely evaluation of hyperacute stroke (22) in humans are considerable, since an entire imaging session need take no more than 5 min. For further research work, the rapidity and ease of acquiring images of adequate quality facilitate far more detailed analyses of the attenuation curve than heretofore. Unambiguous effects have been observed on the MRI signal which are consistent with those predicted to be caused, according to the Le Bihan theory, by the superimposed perfusive motion of blood in capillaries. Further improvements in data analysis may lead to observations of changes in the IVIM parameters associated with brain function.

#### ACKNOWLEDGMENTS

The authors acknowledge the use of the excellent facilities of the NIH In Vivo NMR Center, thank Dr. Chrit Moonen for his helpful advice, and thank Dr. L. Kyle Hedges, Dr. James Pekar, Mr. Joseph Maier, Mr. Robert Vavrek, Mr. D. Despres, and Mr. S. Merritt for invaluable assistance.

## REFERENCES

1. R. TURNER AND R. M. BOWLEY, *J. Phys. E* **19**, 876 (1986).
2. P. MANSFIELD, *J. Phys. C* **10**, L55 (1977).
3. R. TURNER, J. MAIER, R. VAVREK, AND D. LE BIHAN, in "Book of Abstracts: Society of Magnetic Resonance in Medicine, 1989," p. 1123, Society of Magnetic Resonance in Medicine, Berkeley, CA, 1989.
4. R. TURNER, D. LE BIHAN, J. MAIER, R. VAVREK, L. K. HEDGES, AND J. PEKAR, *Radiology* **177**, 407 (1990).
5. R. C. MCKINSTRY, R. M. WEISSKOPF, M. S. COHEN, J. M. VEVEA, K. K. KWONG, R. R. RZEDZIAN, T. J. BRADY, AND B. R. ROSEN, in "Book of Abstracts: Society for Magnetic Resonance Imaging, 1990," p. 5, Society of Magnetic Resonance in Medicine, Berkeley, CA, 1990.
6. E. O. STEJSKAL AND J. E. TANNER, *J. Chem. Phys.* **42**, 288 (1965).
7. R. TURNER, in *Cerebral Blood Flow* (A. Rescigno and A. Boicelli, Eds.), pp. 245, Plenum, New York, 1988.
8. R. TURNER, *GE NMR Instrum. Newslett.* **6**, 4 (1989).
9. R. TURNER AND D. LE BIHAN, *J. Magn. Reson.* **86**, 445 (1990).
10. A. M. HOWSEMAN, M. K. STEHLING, B. CHAPMAN, R. COXON, R. TURNER, R. J. ORDIDGE, M. G. CAWLEY, P. GLOVER, P. MANSFIELD, AND R. E. COUPLAND, *Br. J. Radiol.* **61**, 822 (1988).
11. R. TURNER, *J. Phys. D* **19**, L147 (1986).
12. R. TURNER, *J. Phys. E* **21**, 948 (1988).
13. P. MANSFIELD AND B. CHAPMAN, *J. Magn. Reson.* **66**, 573 (1986).
14. P. B. ROEMER, W. A. EDELSTEIN, AND J. S. HICKEY, in "Book of Abstracts: Society of Magnetic Resonance in Medicine 1986," p. 1067, Society of Magnetic Resonance in Medicine, Berkeley, CA 1986.
15. S. BLACKBAND, J. D. CHATHAM, W. O'DELL, AND S. DAY, *Magn. Reson. Med.* **15**, 240 (1990).
16. D. LE BIHAN AND E. BRETON, *C.R. Acad. Sci.* **15**[II], 1109 (1985).
17. D. LE BIHAN, E. BRETON, D. LALLEMAND, P. GRENIER, E. CABANIS, AND M. LAVAL-JEANTET, *Radiology* **1161**, 401 (1986).
18. D. LE BIHAN, E. BRETON, D. LALLEMAND, M.-L. AUBIN, J. VIGNAUD, AND M. LAVAL-JEANTET, *Radiology* **168**, 497 (1988).
19. M. E. MOSELEY, Y. COHEN, J. KUCHARCZYK, J. MINTOROVITCH, H. S. ASGARI, M. F. WENDLAND, J. TSURUDA, D. NORMAN, AND P. WEINSTEIN, *Radiology* **176**, 439 (1990).
20. T. L. CHENEVERT, J. A. BRUNBERG, AND J. G. PIPE, *Radiology* **177**, 401 (1990).
21. B. R. ROSEN, personal communication (1990).
22. M. E. MOSELEY, J. KUCHARCZYK, J. MINTOROVITCH, *et al.*, *AJNR* **11**, 423 (1990).